Journal of Drug Delivery Science and Technology 88 (2023) 104895

Contents lists available at ScienceDirect

Journal of Drug Delivery Science and Technology

journal homepage: www.elsevier.com/locate/jddst

Hot melt extrusion for enhanced dissolution and intestinal absorption of hydrochlorothiazide

Ebtessam Essa [a,b], Manna Amin [a,c], Amal Sultan [b], Mona Arafa [b], Gamal El Maghraby [b], Christopher McConville [a,*]

[a] School of Pharmacy, Institute of Clinical Sciences, College of Medical and Dental Sciences, University of Birmingham, Edgbaston, B15 2TT, United Kingdom
[b] Department of Pharmaceutical Technology, Faculty of Pharmacy, Tanta University, Tanta, Egypt
[c] Department of Pharmaceutics, Pharmacy of College, Umm Al-Qura University, Makkah, 21955, Saudi Arabia

ARTICLE INFO

Keywords:
Hydrochlorothiazide
Hot melt extrusion
Dissolution enhancement
Intestinal absorption
In situ rabbit intestinal perfusion technique

ABSTRACT

Hydrochlorothiazide (HTZ) is a potent thiazide diuretic that is used in the management of hypertension. However, HTZ suffers from low and variable oral bioavailability owing to its poor dissolution and limited intestinal permeability. Thus, the aim of this study was to enhance the dissolution rate of HTZ using hot melt extrusion (HME). The goal was to employ excipients capable of improving intestinal permeability of HTZ and modulate the physical properties of the extrudate including its disintegration rate. Formulations comprising HTZ, Kollidon® VA 64, Avicel and either Cremophore RH 40 or Poloxamer 188 were prepared using HME. The formulations were characterized using differential scanning calorimetry, X-ray diffraction, scanning electron microscopy and in vitro dissolution testing. The intestinal permeability was assessed using in situ rabbit intestinal perfusion technique. Analysis suggested that HTZ was either molecularly dispersed or in its amorphous form within the formulation. Dissolution testing reflected significant enhancement in HTZ dissolution rate after HME. In situ intestinal absorption studies revealed site dependent absorption of HTZ. The absorption decreased as it moves down the small intestine before increasing again at the colon contrasting the regional expression of P-glycoprotein transporters. Co-perfusion of HTZ with either poloxamer188 or cremophore RH40 improved the intestinal absorption from jejunum and ileum with the enhancement being significant in ileum segment. Intestinal absorption enhancement was associated with a significant increase in HTZ transcellular absorption reflecting modulation of the drug P-glycoprotein efflux and fluidization of the intestinal membrane. This study demonstrates the potential of HME as a tool for enhancing the dissolution and bioavailability of HTZ.

1. Introduction

Hydrochlorothiazide (HTZ) is a potent thiazide diuretic which inhibits the ability of the kidneys to retain water. It is typically used in combination with other cardiovascular drugs in the management of hypertension [1,2]. Hydrochlorothiazide is classified as a class IV drug (poorly soluble and poorly permeable) according to the biopharmaceutical system classification [3]. The oral bioavailability of HTZ is low and variable due to its slow dissolution rate and poor membrane permeability [4]. The solubility of HTZ in aqueous solutions with different pH values is low. It was reported that the solubility of HTZ in pH range from 1.0 to 7.4 ranged from 0.0608 to 0.103 g/100 ml while its solubility in solutions with pH range from 10.2 to 11.6 were from 1.79 to 2.2 g/100 mL [5]. Pharmaceutical formulators have employed several formulation approaches for enhancing the dissolution rate and the oral bioavailability of HTZ. These include co-crystallization with other co-formers (Sanphui and Rajput, 2014; [2,3]. Preparation of different nanosystems such as nanostructured lipid carriers [4], solid lipid nanoparticles [6] and nanoparticles [7]. Incorporation in solid dispersion systems [8,9]. Another approach is the use of a dissolution enhancement technique which can release excipients capable of improving intestinal permeability. Hot melt extrusion (HME) can be used to achieve this and has been employed as an efficient processing method for the development of molecular drug dispersions within different polymer matrices. HME has been utilized for enhancing the dissolution rate and oral bioavailability of poorly water-soluble drugs [10]. The process of HME comprises the compaction and transformation of powder blends to a uniformly shaped extrudate [10,11]. The steps of

* Corresponding author.
E-mail address: c.mcconville.2@bham.ac.uk (C. McConville).

https://doi.org/10.1016/j.jddst.2023.104895
Received 17 April 2023; Received in revised form 13 August 2023; Accepted 28 August 2023
Available online 29 August 2023

HME include melting and forcing the polymers, additives, and the active pharmaceutical ingredient (API) through an orifice (die) with control over the temperature, pressure, screw speed and feeding rate [11].

HME has numerous advantages compared with other conventional pharmaceutical processing approaches. These include enhancing the solubility and bioavailability of poorly water-soluble drugs, solvent-free, it is an economical and continuous process, provides a product with high stability and uniform distribution of the API. In addition, the product can be tailored to provide immediate, sustained, modified, or targeted release based on the polymers used [11–13]. Recently, it was investigated for continuous manufacture of drug products with promising results [14]. Despite these advantages, HME has certain disadvantages which include thermal stability of the API, given the temperature used and a limited number of polymers and excipients available for use [11]. In addition, the hardness of the produced extrudate provides another challenge due to extended disintegration times which can negatively influence the dissolution rate. This may be eliminated by the incorporation of solid carriers which undergo fast disintegration, for example Microcystalline cellulose (Avicel).

The aim of this study was to investigate HME as an approach for the preparation of HTZ extrudate in presence poloxamer 188 and cremophore RH40 for enhanced dissolution and intestinal permeability. Avicel was investigated as a disintegrant, and permeability enhancement was monitored using in situ rabbit intestinal absorption method.

2. Materials and methods

2.1. Materials

Hydrochlorothiazid (HTZ) and Kolliphor®P 188 (Poloxamer 188) were purchased from Sigma Aldrich, USA. Kollidon® VA 64 (Vinylpyrrolidone-vinyl acetate co-polymer) and Cremophore RH 40 is a gift sample from BASF (Ludwigshafen, Germany). Avicel PH 102 (microcrystalline cellulose) was a gift from FMC corp., Pennsylvania, USA.

2.2. Preparation of hot melt extrudates

The composition of the prepared formulations is shown in Table 1. HTZ, Cremophore RH 40 and Avicel PH 102, if present, were homogeneously mixed with Kollidon VA 64 (as carrier) in a mortar and pestle. Each mixture was then fed into the hopper of the extruder using Rondol lab scale 10 mm extruder (Microlab, Rondol Technology Ltd, France). The extruder consisted of co-rotating twin screws and a heating barrel with three heating zones. A 3 mm diameter round opening die was placed at the end of the extrusion barrel. The screw speed was kept at 20 rpm. The operating temperature of the three zones depended on the composition of the mixture and was adjusted based on the rheological properties of each mixture. Rheological behavior was examined using TA instrument Discovery hybrid parallel plate rheometer (Discovery Rheometer, TA instrument, UK). Based on rheological studies, the temperature providing a viscosity value in the range of 10^3 to 10^4 for each combination was used for zone II [15]. Zones I was adjusted at 30 °C below to reduce inconvenient adhesion during feeding, while zone III was adjusted 20 °C below to improve the consistency of the recovered filaments. The extrudates were collected from the die and cooled at room temperature, grounded, and passed through 40 mesh sieves. The obtained solid dispersion powders were stored in a tightly closed containers until further characterization.

2.3. Differential scanning calorimetry (DSC)

The thermal events of pure HTZ, Kollidone VA 64, Avicel PH 102, poloxamer 188 and the HME powders were examined using DSC 25 instrument (TA instruments, UK). Samples ranging from 5 to 9 mg were loaded into aluminum pans and carefully crimped. An empty pan was used as a reference. The reference and test pans were heated from 30 to 400 °C at a heating rate of 10 °C/min, under constant flow of nitrogen gas (50 ml/min).

2.4. Powder X-ray diffraction (PXRD)

PXRD was conducted on pure HTZ, Kollidon VA 64, Avicel PH 102 and the HME powders using a Rigaku Miniflex X-ray diffractometer with Cu Ka radiation ($\lambda = 1.5406$ Å) at 40 KV and 15 mA. The data was collected at ambient temperature between 2θ values of 3–60° with scanning step size set at 0.02°.

2.5. Scanning electron microscopy (SEM) analysis

The morphology of the pure HTZ, Kollidon VA 64, Avicel PH 102 and selected extrudates were monitored using SEM (Jeol 6060, Oxford Inca EDS). Prior to examination, the samples were coated using sputter gold coater and placed in the SEM vacuum chamber.

2.6. HPLC analysis

HTZ analysis was conducted using HPLC (DIONEX, Thermo Scientific, USA). The instrument was equipped with Dionex Ultimate 3000 autosampler with a quaternary gradient pump and Chromeleon Chromatography Data system (CDS). The system was equipped with a variable wavelength UV detector (VWD 1260) and an automatic sampling system (TCC 1260). Separation was performed using reversed phase C18 column 150 × 4.6 mm with an average particle size of 5 μm (Thermo Scientific, USA). The mobile phase comprised a mixture of 0.04 M potassium dihydrogen phosphate buffer adjusted to pH value of 3.0 (using *ortho*-phosphoric acid) and acetonitrile at a 70:30 ratio [2]. The collected samples were loaded into HPLC vials, and the injection volume was 20 μl at a flow rate of 1.0 ml/min with the effluent being analysed at 210 nm. The method was validated for linearity, selectivity, precision and lower limit of quantification (LOQ). The linear calibration range for the detection of HTZ was performed in the concentration range from 10 to 50 μg/mL, with a coefficient of (R^2) of 0.9997 and regression equation of x = 0.6489–0.103.

2.7. In vitro dissolution

The dissolution of HTZ-loaded HME powders was conducted using USP dissolution apparatus type II (Copley, NG 42 JY, Nottingham, UK).

Table 1
Compositions of the prepared formulations and operating temperature in different zones of the extruder.

Formula	Composition of different formulations					Extruder temperature (°C)		
	HTZ	Avicel	Cremophore RH 40	Poloxamer 188	Kollidon VA 64	Zone I	Zone II	Zone III
F1	1	-	1	-	8	130	160	140
F2	1	1	1	-	7	140	170	150
F3	1	1.5	1	-	6.5	140	170	150
F4	1	1.5	-	1	6.5	160	190	170
PM1	1	1.5	1	-	6.5	-	-	-
PM2	1	1.5	-	1	6.5	-	-	-

The dissolution of pure HTZ (as control) and physical mixtures of formulations F3 (PM 1) and F4 (PM 2) were also investigated. Amounts equivalent to 50 mg of HTZ were used. The dissolution medium comprised of 1000 ml of 0.1 N HCl at 37 °C [3]. The paddles were rotated at 50 rpm speed. 5 ml samples were withdrawn at 5, 10, 15, 30, 45 and 60 min and replaced by an equal volume of fresh dissolution medium. The samples were filtered using a 0.45 μm Millipore filter. Drug concentration was determined using HPLC. The dissolution profiles were constructed by plotting the cumulative amounts of HTZ dissolved versus time. These profiles were used to determine the dissolution parameters that was represented as the amount of HTZ dissolved after 5 min (Q5) as well as the dissolution efficiency (DE%). The later was deduced according to the reported calculation protocol by Ref. [9].

2.8. In situ intestinal permeability studies

The effect of the polymers employed in the preparation of HME powders on intestinal HTZ permeability was investigated. This involved preparation of solutions incorporating HTZ with either poloxamer 188 or cremophore RH 40 at the weight ratio (1:1) used during HME. The aqueous HTZ solution was prepared at a concentration of 12.5 μg/ml in phosphate buffered saline (PBS). This was employed as a control perfusion solution which was pH-adjusted according to the exposed intestinal segments for perfusion. All the prepared solutions were warmed to body physiological temperature (37 ± 0.5 °C) just prior to intestinal perfusion experiments.

Male albino rabbits (12 rabbits) weighing approximately 2–2.5 kg were employed for this study. The animals were used following an ethically approved study protocol from College of Pharmacy Ethical Committee, Tanta University (Approval Code, TP/RE/2/23P-009). The surgical procedures adopted for exposing and handling the intestinal segments of interest were taken from the literature [16,17]. In brief, the rabbits were given a pre-anaesthetic intramuscular injection of xylazine hydrochloride. The rabbits were fully anaesthetized using an intramuscular dose of ketamine hydrochloride (45 mg/kg) which was injected 10 min later. An extra ketamine hydrochloride dose of 25 mg/kg was used when required. The rabbit was then supinely laid for pre-surgical preparation and shaving of the belly area. A midline abdominal cut was made to reveal the intestinal segments of interest. The segments were duodenum, jejunum, ileum and colon of 20, 30, 30 and 10 cm length, respectively. Each of the accessed intestinal segments was cannulated proximally using a 3-way stopcock canula and distally using an L-shaped glass canula. These segments were finally arranged in S-shaped pattern after carful cleansing using warm phosphate buffered saline (PBS). The biological viability of the perfused segments was preserved throughout the whole study via intermittent wetting of a gauze pad covering the exposed segments with warm PBS (37 ± 0.5 °C). The formerly prepared HTZ solutions were pumped through the intestinal segments of interest at constant rate (0.27 ml/min) using Harvard-22 perfusion Apparatus, Millis, MA, USA. Each rabbit was utilized for tracking drug absorption from two intestinal segments, simultaneously. The intestinal outflowing perfusate was collected at 10-min intervals for 2 h. The drained samples were volumized, centrifuged immediately and decanted for supernatant drug analysis using HPLC. The procedures were finalized with rabbit euthanasia and precise measurement of the actual length of the perfused segments [18].

2.9. Data analysis

2.9.1. Drug absorptive clearance

Detailed data analysis is available elsewhere in previous investigations [18]. Calculation of HTZ fraction absorbed (Fa) and absorptive clearance (PeA) were achieved using the steady state time points (during the second hour of perfusion). The Fa was computed from the ratio of the outflux to influx drug concentration ($C_{(out)}/C_{(in)}$)ss, both normalized to the intestinal water flux according to equation (1).

$$Fa = 1 - [(C(out) / C(in))ss] \quad (1)$$

The outflow rate of perfusion solution was estimated based on the actual drained samples' volume and the pre-determined sampling time intervals (10 min). Averaging of the outflow rate with the inflow rate (0.27 ml/min) provides the average flow rate (Q) of the perfused solution. The absorptive clearance of HTZ (PeA) in ml/min can be approximated from the fraction remaining of the drug ($C_{(out)}/C_{(in)}$)ss and the average flow rate (Q) using the following equations:

$$PeA = -Q \times \ln(C(out) / C(in))ss \quad (2)$$

$$(C(out) / C(in))ss = e^{-PeA/Q} \quad (3)$$

Where, Pe is the apparent drug permeability coefficient in cm/min and A is the absorptive surface area in cm^2.

Because of the logarithmic nature of drug absorptive clearance exposed in the previous equation, HTZ concentration in the intestinal lumen will never reach absolute zero. Thus, researchers valued a 5% remaining fraction of the drug to express almost complete drug absorption. This will occur at the intestinal length ($L_{95\%}$) which was computed by substitution into equation (3) as follows:

$$0.05 = e^{-PeA.L95\%/Q} \quad (4)$$

Where, PeA is the absorptive clearance normalized to the intestinal length, and $L_{95\%}$ is the length required for 95% drug absorption.

The anatomical remaining length (ARL) of the intestinal segments after approximately complete drug absorption can be calculated by subtracting the $L_{95\%}$ from the maximum length of the explored anatomical site.

2.9.2. Estimation of the drug absorption pathways

The overall drug absorption is a summative contribution of both diffusive and convective transport pathways. The involvement of those pathways in the intestinal drug absorption per unit time (Js) can be translated into the following equation in which {K_S(C- Cp)} presents the diffusive contribution while {$\Phi_S J_w C$} denotes the convective contribution:

$$J_S = K_S(C - C_p) + \Phi_S J_w C \quad (5)$$

Where, K_S is the diffusive permeability constant, Φ_S is the sieving constant, J_w is the overall estimated water flux, C is the intestinal drug concentration and, C_p is the plasma concentration of the drug. Shortening of the last equation is acceptable at steady state due to the blood sink conditions as follows:

$$J_{ss} = K_s C_{ss} + \Phi_s J_w C_{ss} \quad (6)$$

$$J_{ss}/C_{ss} = K_s + \Phi_s J_w \quad (7)$$

J_{ss} and C_{ss} are the drug flux and the drug concentration in intestinal lumen at steady state, respectively. J_{ss}/C_{ss} implies the overall absorption of the drug irrespective to the membrane transport pathway which can be experimentally appraised as (PeA). Based on Equation (7), graphical presentation of the drug absorptive clearance (PeA) as a function of the water flux (J_w) provides a line, the slope of which is Φ_s while the intercept with the Y- axis is K_s. Dividing the later upon the overall drug absorptive clearance and expressing as percentage affords an estimation of the % transcellular HTZ absorption with the complementary being taken for the % paracellular absorption estimation.

3. Results and discussion

3.1. Differential scanning calorimetry (DSC)

DSC experiments were conducted to assess the thermal behavior of

HTZ in the pure state and after formulation via HME (Fig. 1). The thermogram of pure HTZ showed a sharp endothermic peak at 274.8 °C. This endothermic peak can be attributed to HTZ melting and reflects its crystallinity. The thermogram also revealed a broad exothermic peak at 315.2 °C which can be credited to drug decomposition (Fig. 1). Previous research has reported a similar thermal pattern for HTZ (Martins et al., 2012; [2,3].

For Kollidon VA 64, the thermogram displayed a glass transition temperature at 111.5 °C and an endothermic peak at 323.3 °C which can be accredited to its decomposition (Fig. 1). This thermal behavior correlated with that reported in literature [19]: [10]. The thermogram of Avicel PH 102 showed a broad endothermic peak with an onset of 36.5 °C and end of 144.8 °C which corresponds to evaporation of adsorbed water. Another peak was recorded at 329.4 °C and can be credited to melting of the avicel followed by decomposition (Fig. 1). Similar thermograms have been reported previously for avicel PH 102 [20]. The DSC thermogram of poloxamer 188 showed a sharp melting endotherm at 49.7 °C (Fig. 1). This thermal behavior is similar to that obtained in the literature [21]; Essa et al., 2017).

With respect to the HME formulations, the main melting endotherm of HTZ completely disappeared in all formulations (Fig. 1). This indicates solubilization of the drug in the melted polymers or its existence in an amorphous form. A similar explanation was provided by Refs. [10, 22]. A broad decomposition endothermic peak was recorded at 323.3 °C in all formulations which can be attributed to the existence of Kollidon VA 64. A melting endotherm was recorded at 48.3 °C in the formulation containing poloxamer 188 (F4). Noteworthy, the thermograms of physical mixtures showed absence of the endothermic transition of HTZ. This indicates solubilization of the drug in the melted polymer upon progressive heating. Similar behavior was shown in physical mixtures and was similarly explained by other investigators [21].

3.2. Powder X-ray diffraction (PXRD)

The X-ray diffraction patterns of pure HTZ, polymers and the HME formulations are shown in Fig. 2. The diffraction pattern of HTZ shows its typical diffraction peaks at 2θ values of 10.5, 17.4, 19.9, 21.9, 22.4, 29.8, 36.9, 38.5, 42.9 and 47.9° confirming the crystalline nature of the drug. This data correlated with the obtained DSC thermogram of HTZ and is similar to that reported in the literature [2,3,8]. The diffractogram of kollidon VA 64 showed no diffraction peaks verifying its amorphous nature [23]. The crystallinity of avicel PH 102 was shown to have numerous diffraction peaks appearing at 2θ values of 16.4, 23.6, 31.6, 38.1 and 44.3° [24,25]. The diffractogram of poloxamer reflects its characteristic crystalline structure which is similar to that reported in other studies [26].

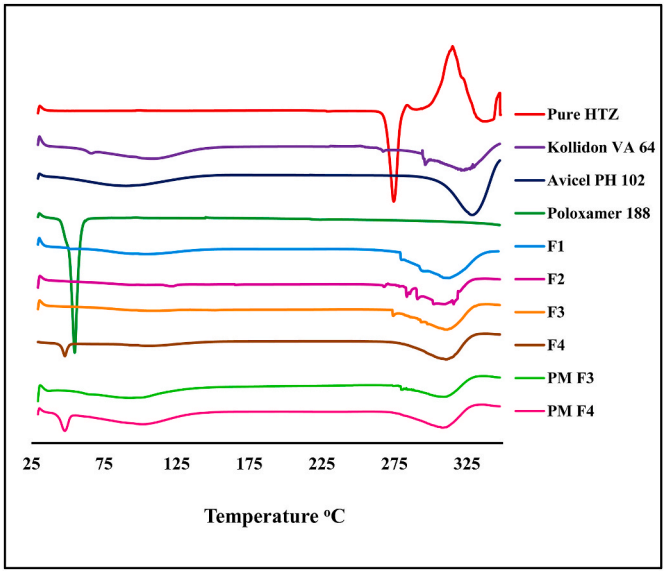

Fig. 1. Thermograms of unprocessed HTZ, Kollidon VA 64, Avicel PH 200, poloxamer 188, physical mixtures and the prepared formulations.

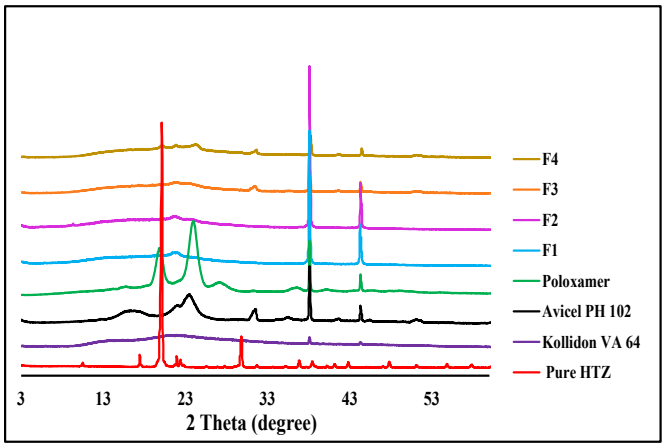

Fig. 2. X-ray diffractograms of unprocessed HTZ, Kollidon VA 64, Avicel PH 200, poloxamer and their formulations.

Regarding the HME formulations, the characteristic diffraction peaks of HTZ disappeared with the diffraction peaks of avicel PH 102 dominating the diffractograms (Fig. 2). These data indicate the solubilization of HTZ in the polymer or that it is its amorphous form. These results correlate with the DSC data and the literature [27,28].

3.3. Scanning electron microscopy (SEM) analysis

The morphology of HTZ, avicel PH 102, kollidon VA 64 and the optimum HME formulations was investigated using SEM with the recorded micrographs presented in Fig. 3. The micrographs show large and irregular crystals of HTZ which is commonly reported in literature [7,29]. Avicel was shown with non-spherical angular shape particles of variable size [30,31], while kollidon VA 64 revealed hollow spherical particles with some broken fragments [32]. Noticeable changes were observed in the micrographs of the HME formulations. For example, F3 had uniform particles of reduced size while in case of F4 the particles were relatively large. Both formulations showed particles with irregular texture which is different from that recorded for the individual components of each formulation. These findings reflect homogenous distribution of the drug in the polymers. Similar findings were recorded for other drugs after HME and the authors took this as a reflection for amorphization. This explanation is applicable to our findings which is supported by the recorded x-ray data [19,33].

3.4. In vitro dissolution

Dissolution studies were conducted to assess the impact of the preparation of HTZ solid dispersions by HME on its dissolution rate (Fig. 4). The calculated dissolution parameters including the amount dissolved in the first 5 min (% Q5) and percent dissolution efficiency (% DE) are presented in Table 2. The dissolution profile of pure HTZ revealed a slow dissolution rate with a % Q5 of 20.5 ± 1.1%. This slow dissolution rate was further supported with a % DE of 67.4 ± 1% [2,3]. The HME formulations resulted in a significant enhancement in the HTZ dissolution rate ($P < 0.05$) (Fig. 4) and confirmed by an increase in both the % Q5 and % DE values (Table 2). The % Q5 values were 62.5 ± 1.6%, 80.1 ± 0.9% and 94.5 ± 1.1% for F1, F2 and F3, respectively. The degree of enhancement is correlated with the ratio of avicel used in the HME formulations. This can be explained based on the ability of avicel to increase the disintegration rate of the extrudate allowing for faster

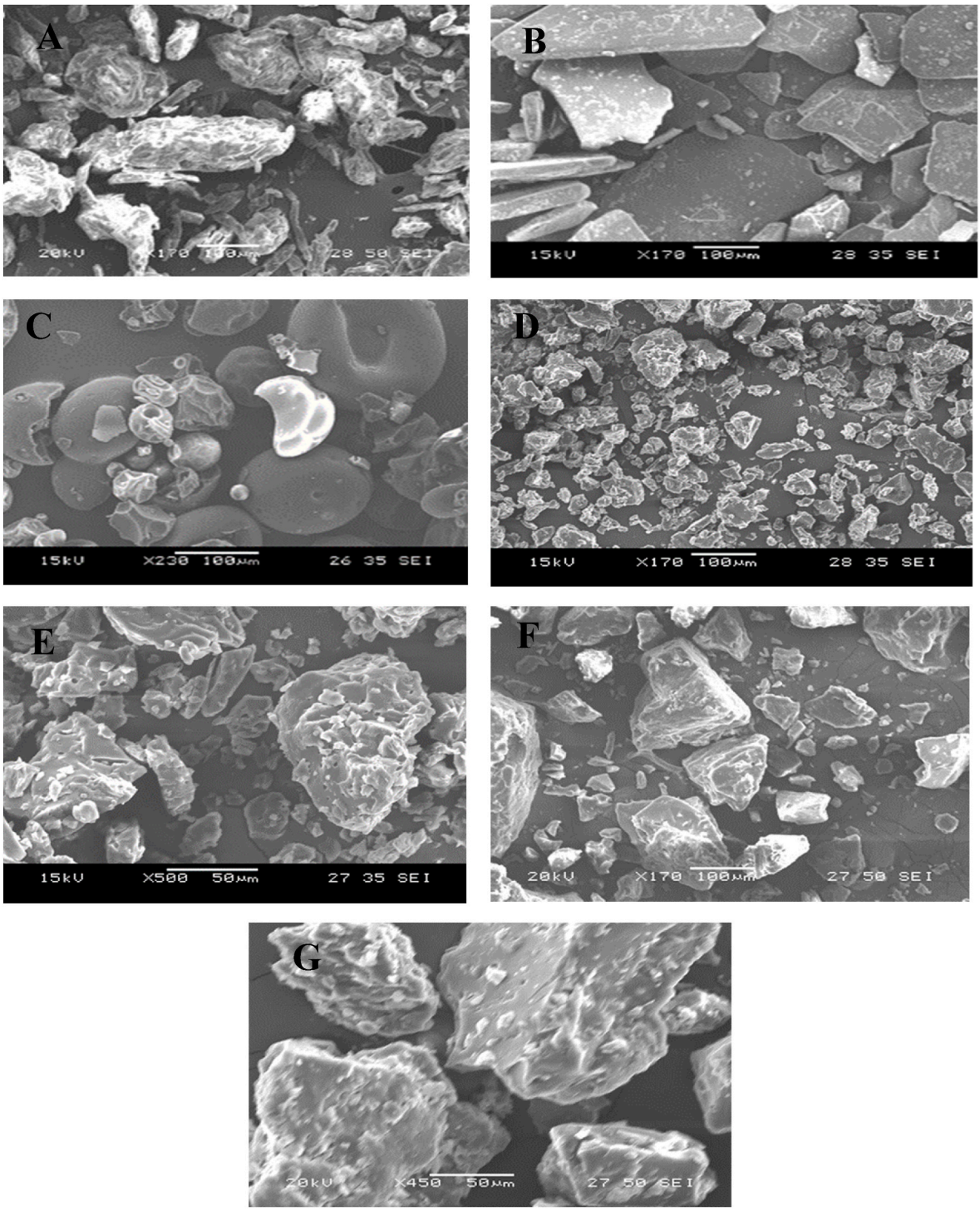

Fig. 3. Scanning electron microscope pictures of Avicel (A), HTZ (B), Kollidon VA 64 (C), Formula F3 at low (D) and high (E) magnification, and formula F4 at low (F) and high (G) magnification.

liberation of primary particles which undergo faster dissolution. Incorporation of poloxamer 188 instead of cremophore RH 40 in F4 resulted in % Q 5 value of 79.8 ± 4.4 and % DE value of 85.6 ± 1.7 which are significantly higher than that were recorded for pure drug ($P < 0.05$). Noteworthy, recording almost 100% dissolution in the optimized formulation reflects absence of drug degradation during processing. It is important to emphasize that, the rank of dissolution enhancement from different formulations remained the same when considering Q10 and Q15 as additional dissolution parameters (Table 2). The enhancement in the dissolution rate of HTZ after HME can be accredited to drug amorphization and/or solubilization in the employed polymers as revealed from the DSC and X-ray data. The impact of HME on enhancing drug dissolution rate was confirmed from the recorded dissolution profiles of drug polymer physical mixture (Fig. 4). The corresponding physical mixtures reduced the dissolution rate when compared to pure HTZ. This reduction is probably due to possible aggregation of the drug with the formulation components upon physical mixing. HME has been previously shown as an efficient approach for enhancing the dissolution rate of poorly water-soluble drugs [34–36]. Noteworthy, the recorded dissolution studies employed 0.1 N HCl to ensure immediate dissolution

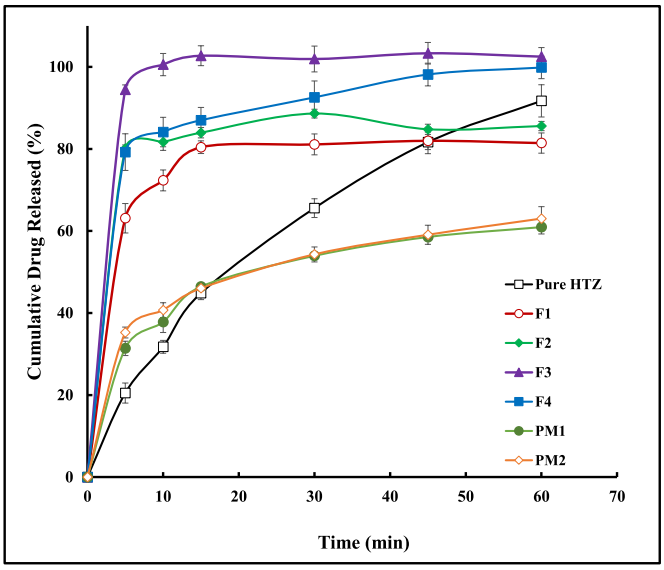

Fig. 4. Dissolution profiles of the prepared HTZ formulations and unprocessed drug. For formulation details refer to Table 1.

Table 2
The calculated dissolution parameters of the prepared formulations.

Formula	Q5 (%)	Q10 (%)	Q15 (%)	% DE
HTZ (Control)	20.5 ± 1.1 (5.4)	31.8 + 1.6 (5)	44.8 + 0.9 (2)	67.4 ± 1 (1.5)
F1	62.5 ± 1.6 (2.6)	72.5 + 1.3 (1.8)	79.9 + 2.4 (3)	77.9 ± 6.3 (8)
F2	80.1 ± 0.9 (1.1)	81.5 + 2.5 (3.1)	84 + 1.5 (1.8)	81.2 ± 1.4 (1.7)
F3	94.5 ± 1.1 (1.2)	100.6 + 2.7 (2.7)	102.7 + 6.3 (6.1)	93.8 ± 3.1 (3.3)
F4	79.8 ± 4.4 (5.5)	85.3 + 3.6 (4.2)	88.7 + 3.1 (3.5)	85.6 ± 1.7 (1.9)
PM1	31.4 ± 0.9 (2.9)	37.8 + 0.13 (0.34)	46.4 + 1.2 (2.6)	60.5 ± 1.6 (2.6)
PM2	35.2 ± 1.7 (4.8)	40.7 + 0.8 (2)	46.7 + 0.6 (1.3)	61.5 ± 0.3 (0.49)

Values represent mean ± SD (n = 3).
Values between brackets represent % relative standard deviation (% RSD).

in the stomach. Taking the pH dependent solubility of HTZ into consideration, better dissolution will be expected at higher pH values in the small intestine [5]. This will allow any undissolved drug to undergo fast liberation after transfer from stomach to intestine. This can add to the expected performance of the fabricated systems.

3.5. *In situ intestinal permeability studies*

The intestinal membrane transport of the unprocessed HTZ and the probable mechanisms underlying its permeation were explored. Additionally, the effect of permeation enhancing polymers in the HME formulations on HTZ permeability was also investigated. The rabbit in situ intestinal perfusion technique is a reliable absorption predictive model. The merits of such technique have been covered in literature [16,37]. One of which is the preservation of the intestinal tissue viability due to maintained blood and nerve supply throughout the whole study. The influence of food on intestinal drug absorption can be omitted using this technique. Moreover, the effect of either gastroparesis or gastric dumping on the drug absorption is fully excluded. Regarding the choice of animal, the selection of albino rabbits was based on the physiological resemblance to humans which further complements the advantages of the technique [38].

3.5.1. *Intestinal region-dependent absorption of HTZ*

The intestinal absorption of the unprocessed HTZ was inspected at four intestinal anatomical sites; duodenum, jejunum, ileum and colon. The recorded HTZ absorption parameters from its control perfusion solution (12.5 μg/ml) are presented in Table 3. The data reflected poor intestinal permeability of HTZ from the four intestinal anatomical sites. This was demonstrated by the calculated percent fraction absorbed of the drug normalized to segment length (%Fa/L) and the low HTZ absorptive clearance (PeA/L). Notably, the estimated length required for almost complete drug absorption ($L_{95\%}$) exceeded the maximum anatomical length of the examined segments with subsequent calculated negative anatomical remaining length (ARL) values. This indicated the incomplete intestinal absorption of HTZ, which complies with its reported classification as a BCS class IV drug [3]. The recorded results correlate with the published data for HTZ which employed a similar strategy [38]. Interestingly, the recorded parameters highlighted the dependence of HTZ intestinal absorption at steady state on the anatomical site. This was manifested from the significant ranking of HTZ absorption from colon< duodenum< jejunum< ileum (Table 3). The ranking correlates closely the regional expression of intestinal P-glycoprotein (P-gp) efflux transporters and may suggest the role of P-gp transporters in limiting the intestinal permeability of HTZ [39]. Previous studies have pointed to the potential effect of a P-gp inhibitor to enhance the membrane transport of HTZ both in vitro using caco-2 cells monolayers and in situ employing closed loop intestinal perfusion [40]. Utilization of the in situ intestinal perfusion technique to provide an evidence for the P-gp efflux of drugs, based on the site-dependent absorptive clearance has previously been reported [39].

Estimation of the relative contribution of transcellular and paracellular absorptive pathways was conducted via monitoring the effect of water flux on the drug absorptive clearance at steady state (Fig. 5). The data revealed a dominant contribution of the paracellular pathway to HTZ absorption from the four intestinal segments (Table 4). This contribution was even augmented from colon segment (99.8%). Similar observations have been reported previously for HTZ and was attributed to the intervention of the pharmacodynamic diuretic effect of HTZ [38]. This necessitates cautious consideration of the increased water flux in the GIT which confuses proper estimation of the contribution of absorptive pathways based on the water flux. Another diuretic drug, furosemide behaved similarly after monitoring its intestinal absorption using in situ intestinal perfusion technique [41].

3.5.2. *Effect of HMEs coupled polymers on intestinal absorption of HTZ*

The effect of poloxamer 188 and cremophore RH40 on intestinal absorption of HTZ was monitored. This involved co-perfusion of HTZ with either poloxamer 188 or cremophore RH40 through jejunum and ileum segments. The recorded absorption parameters are presented in Table 5. Co-perfusion of HTZ with poloxamer 188 resulted in enhancement of intestinal absorption from both jejunum and ileum segments, with an increased hastened drug absorptive clearance and %Fa/L from both segments as well as a decrease of the approximated $L_{95\%}$ (Table 5). The permeation enhancing potential of poloxamer 188 has previously

Table 3
The calculated intestinal permeation parameters of hydrochlorothiazide.

Parameter	Duodenum	Jejunum	Ileum	Colon
%Fa/L	2.6 ± 0.3	1.2 ± 0.2	0.8 ± 0.1	3.3 ± 0.4
PeA/L (ml/min.cm)	0.0076 ± 0.0010	0.0034 ± 0.0006	0.0023 ± 0.0003	0.0089 ± 0.0008
$L_{95\%}$ (cm)	100.5 ± 25.0	287.2 ± 65.3	351.1 ± 66.7	85.5 ± 4.7
ARL	−80.5 ± 25.0	−167.2 ± 65.3	−291.1 ± 66.7	−70.5 ± 4.7
J_w/L (ml/min. cm)	0.0059 ± 0.0004	0.0026 ± 0.0011	0.0018 ± 0.0002	0.0095 ± 0.0015

Values represent mean ± SD (n = 3).

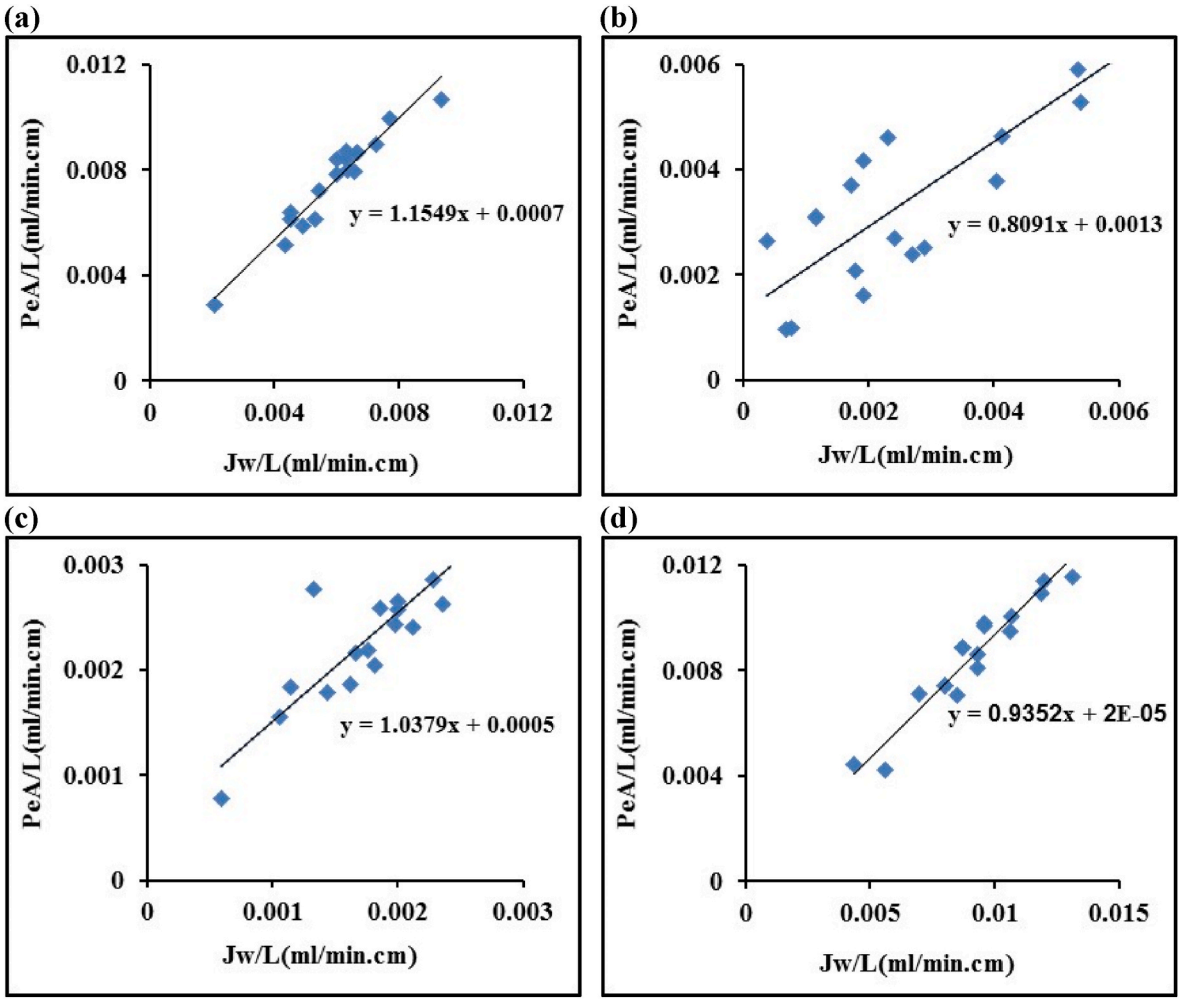

Fig. 5. Effect of the length normalized water flux (Jw/L) on the absorptive clearance (PeA/L) of HTZ in duodenum (a), jejunum (b), ileum (c), and colon (d).

Table 4
The estimated contribution of absorptive pathways expressed as percentage to hydrochlorothiazide (HTZ) absorption in absence and presence of the selected polymers.

	Duodenum	Jejunum	Ileum	Colon
Control HTZ solution				
Transcellular pathway (%)	9.3	37.9	21.7	0.2
Paracellular pathway (%)	90.7	62.1	78.3	99.8
HTZ/Poloxamer188 solution				
Transcellular pathway (%)	-	75.2	79.9	-
Paracellular pathway (%)	-	24.8	20.1	-
HTZ/Cremophore solution				
Transcellular pathway (%)	-	50.4	49.4	-
Paracellular pathway (%)	-	49.6	50.6	-

Table 5
The calculated intestinal permeation parameters of hydrochlorothiazide (HTZ) in the presence of the selected polymers.

Parameter	HTZ/Poloxamer188 solution		HTZ/Cremophore solution	
	Jejunum	Ileum	Jejunum	Ileum
%Fa/L	1.3 ± 0.2	1.2** ±0.1	1.1 ± 0.2	1.3* ±0.3
PeA/L (ml/min.cm)	0.0039 ± 0.0008	0.0034* ±0.0003	0.0032 ± 0.0005	0.0039 ± 0.0011
$L_{95\%}$ (cm)	197.2 ± 43.7	287.2* ± 65.3	243.3 ± 30.5	196.3* ±50.5
ARL	−77.2 ± 43.7	−167.2* ±65.3	−123.3 ± 30.5	−136.3* ±50.5
J_w/L (ml/min. cm)	0.0022 ± 0.0009	0.0023 ± 0.0018	0.0021 ± 0.0005	0.0033* ±0.0007

Values represent mean ± SD (n = 3).
*Significant difference from control HTZ parameters (P < 0.05).
**Significant difference from control HTZ parameters (P < 0.01).

been reported [42]. Interestingly, the enhancement of HTZ absorption after co-perfusion with poloxamer 188 was significant ($P < 0.05$) in ileum while being recorded only as a trend in jejunum (Table 5). This together with the reported P-gp inhibitory effect of poloxamer 188 as the main mechanism underlying its nature as a permeation enhancer could provide further confirmation for the contributing role of P-gp to the limited HTZ permeability [42–44]. Additionally, the effect of water flux on the absorptive clearance of HTZ was investigated in the presence of the selected polymers to provide an estimate of the relative contribution to the absorptive pathways (Fig. 6). Notably, the recorded absorption enhancement in presence of poloxamer 188 was associated with an increase in the contribution of the transcellular pathway to HTZ absorption from both the jejunum and ileum segments (Table 4). This was increased from 37.9% to 75.2% and from 21.7% to 79.9% in jejunum and ileum, respectively. Augmented contribution of transcellular absorption of P-gp substrates after in situ co-perfusion with a P-gp inhibiting excipients or drug delivery systems has been previously reported [18,39]. Furthermore, induced momentary loosening of the tight junctions and membrane fluidizing effects of poloxamer 188 may have a direct impact facilitating HTZ membrane transport [45,46].

Similarly, incorporation of cremophore RH40 in the HTZ perfusion

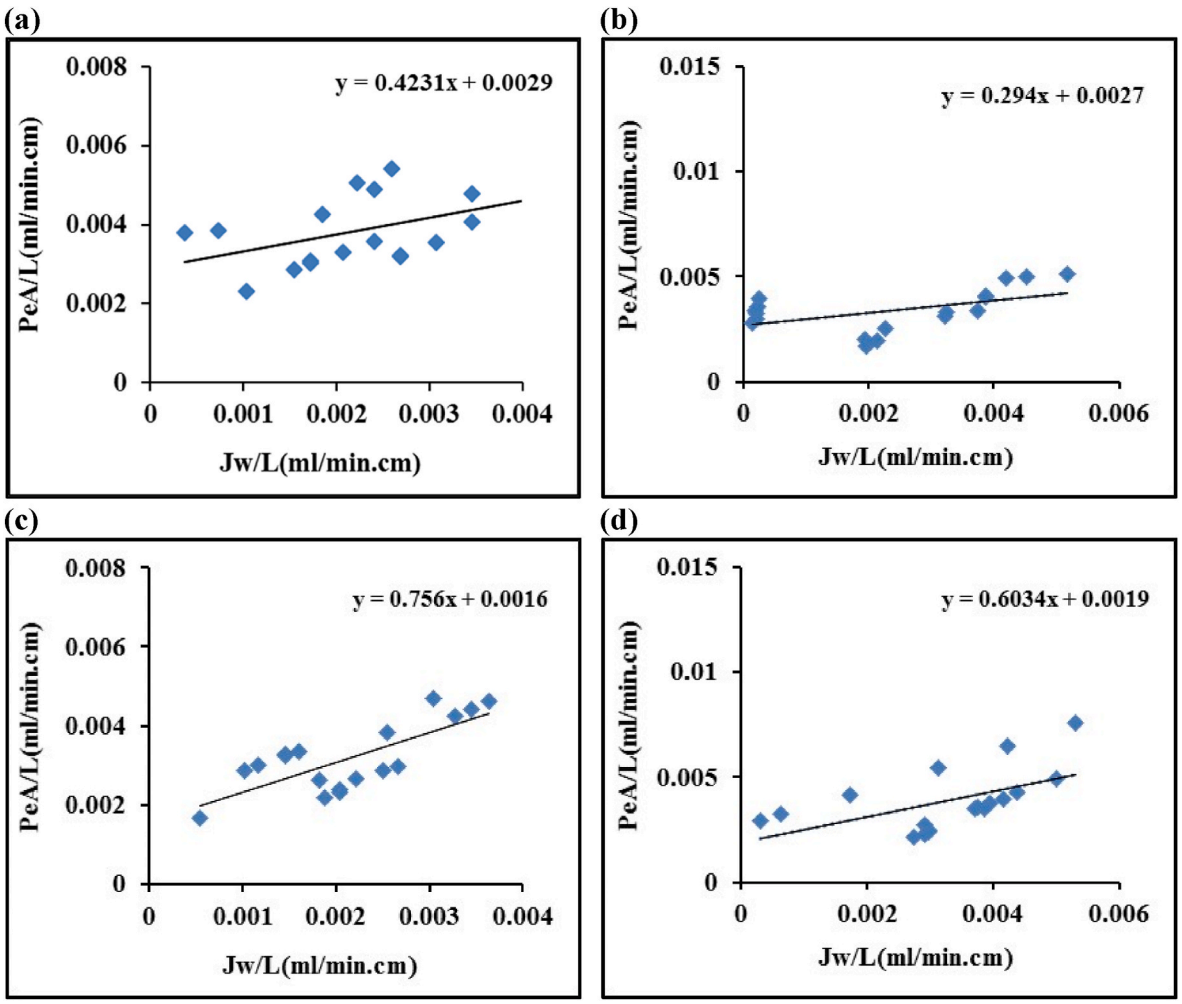

Fig. 6. Effect of the length normalized water flux (Jw/L) on the absorptive clearance (PeA/L) of HTZ in presence of poloxamer 188 in jejunum (a), ileum (b), and in presence of cremophore in jejunum (a) and ileum (b).

solution resulted in enhancement of HTZ absorption from both jejunum and ileum with the enhancement being more dominant in ileum segment (Table 5). Investigation of the effect of water flux on the absorptive clearance of HTZ in presence of cremophore RH40 revealed an increased involvement of the transcellular pathway from both segments (Fig. 6, Table 4). Cremophore-induced alteration of the intestinal membrane fluidity may provide an explanation for the enhancement in HTZ absorption [47]. Additionally, cremophore RH40 has been reported to potentially inhibit P-gp transporters with subsequent improvement of intestinal permeation of P-gp substrates [47,48]. The later mechanism combined with the improved HTZ absoprtion in ileum segment is supported by the higher ileum expression of P-gp transporters [18,39].

4. Conclusion

HTZ was successfully formulated using HME, increasing its dissolution rate. The drug exists within these formulations as either a dispersion within the polymers or an amorphous solid. Intestinal absorption of HTZ is limited by P-glycoprotein efflux transporters. Significant enhancement of HTZ intestinal absorption was recorded after co-perfusion with the polymers used in the HME formulations. The use of HME to formulate HTZ into dosage oral dosage forms containing Avicel, Kollidon VA 64 and either poloxamer 188 or cremophore RH40 has the potential to significantly improve its bioavailability via an improvement in both its dissolution and absorption.

Author contributions

Ebtessam Essa and Manna Amin conducted the preparation and characterization of the hot melt extrudates. Amal Sultan, Mona Arafa and Gamal El Maghraby assisted with experimental design. Ebtessam Essa and Christopher McConville designed and supervised all of the experiments and wrote the manuscript with all authors contributing.

Declaration of competing interest

The authors declare that they have no known competing financial interests or personal relationships that could have appeared to influence the work reported in this paper.

Data availability

Data will be made available on request.

References

[1] S.G. Chrysant, M.A. Weber, A.C. Wang, D.J. Hinman, Evaluation of antihypertensive therapy with the combination of olmesartan medoxomil and hydrochlorothiazide, Am. J. Hypertens. 17 (2004) 252–259, https://doi.org/10.1016/j.amjhyper.2003.11.003.

[2] M.F. Arafa, S.A. El-Gizawy, M.A. Osman, G.M. El Maghraby, Sucralose as co-crystal co-former for hydrochlorothiazide: development of oral disintegrating tablets, Drug Dev. Ind. Pharm. 42 (2016) 1225–1233, https://doi.org/10.3109/03639045.2015.1118495.

[3] S.A. El-Gizawy, M.A. Osman, M.F. Arafa, G.M. El Maghraby, Aerosil as a novel co-crystal co-former for improving the dissolution rate of hydrochlorothiazide, Int. J. Pharm. 478 (2015) 773–778, https://doi.org/10.1016/j.ijpharm.2014.12.037.

[4] M. Cirri, L. Maestrini, F. Maestrelli, N. Mennini, P. Mura, C. Ghelardini, L. Di Cesare Mannelli, Design, characterization and in vivo evaluation of nanostructured lipid carriers (NLC) as a new drug delivery system for hydrochlorothiazide oral administration in pediatric therapy, Drug Deliv. 25 (2018) 1910–1921, https://doi.org/10.1080/10717544.2018.1529209.

[5] S.A. Urek Blatnik, R. Dreu, S. Srčič, Influence of pH modifiers on the dissolution and stability of hydrochlorothiazide in the bi-and three-layer tablets, Acta Pharm. 31 (4) (2015) 383–397, 65.

[6] M. Cirri, N. Mennini, F. Maestrelli, P. Mura, C. Ghelardini, L.D. Mannelli, Development and in vivo evaluation of an innovative "Hydrochlorothiazide-in Cyclodextrins-in Solid Lipid Nanoparticles" formulation with sustained release and enhanced oral bioavailability for potential hypertension treatment in pediatrics, Int. J. Pharm. 521 (2017) 73–83, https://doi.org/10.1016/j.ijpharm.2017.02.022.

[7] E. Vaculikova, A. Cernikova, D. Placha, M. Pisarcik, P. Peikertova, K. Dedkova, F. Devinsky, J. Jampilek, Preparation of hydrochlorothiazide nanoparticles for solubility enhancement, Molecules 21 (2016) 1005, https://doi.org/10.3390/molecules21081005.

[8] R.V. Trivedi, P.S. Admane, J.B. Taksande, J.G. Mahore, M.J. Umekar, Solubility enhancement studies of hydrochlorothiazide by preparing solid dispersions using losartan potassium and urea by different methods, Der Pharm. Lett. 3 (2011) 8–17.

[9] A. Khan, Z. Iqbal, Y. Shah, L. Ahmad, Z. Ullah, A. Ullah, Enhancement of dissolution rate of class II drugs (Hydrochlorothiazide); a comparative study of the two novel approaches; solid dispersion and liqui-solid techniques, Saudi Pharmaceut. J. 23 (2015) 650–657, https://doi.org/10.1016/j.jsps.2015.01.025.

[10] J.M. Vasoya, H.H. Desai, S.G. Gumaste, J. Tillotson, D. Kelemen, D.M. Dalrymple, A.T. Serajuddin, Development of solid dispersion by hot melt extrusion using mixtures of polyoxylglycerides with polymers as carriers for increasing dissolution rate of a poorly soluble drug model, J. Pharmaceut. Sci. 2019 (108) (2019) 888–896, https://doi.org/10.1016/j.xphs.2018.09.019.

[11] M. Maniruzzaman, J.S. Boateng, M.J. Snowden, D. Douroumis, A review of hot-melt extrusion: process technology to pharmaceutical products, ISRN Pharm 2012 (2012), 436763, https://doi.org/10.5402/2012/436763.

[12] R. Chokshi, H. Zia, Hot-melt extrusion technique: a review, Int. J. Psychol. Res. 31 (2004) 3–16, https://doi.org/10.22037/ijpr.2010.290.

[13] C. McConville, P. Tawari, W. Wang, Hot melt extruded and injection moulded disulfiram-loaded PLGA millirods for the treatment of glioblastoma multiforme via stereotactic injection, Int. J. Pharm. 494 (2015) 73–82, https://doi.org/10.1016/j.ijpharm.2015.07.072.

[14] V. De Margerie, C. McConville, S.M. Dadou, S. Li, P. Boulet, L. Aranda, A. Walker, V. Mohylyuk, D.S. Jones, B. Murray, G.P. Andrews, Continuous manufacture of hydroxychloroquine sulfate drug products via hot melt extrusion technology to meet increased demand during a global pandemic: from bench to pilot scale, Int. J. Pharm. 605 (2021), 120818, https://doi.org/10.1016/j.ijpharm.2021.120818.

[15] S.S. Gupta, A. Meena, T. Parikh, T.M. Abu, A.T.M. Serajuddin, Investigation of thermal and viscoelastic properties of polymers relevant to hot melt extrusion - I: polyvinylpyrrolidoneand related polymers, J. Excipients Food Chem. 5 (1) (2014) 32–45.

[16] M.A. Osman, G.M. El Maghraby, M.A. Hedaya, Intestinal absorption and presystemic disposition of sildenafil citrate in the rabbit: evidence for site-dependent absorptive clearance, Biopharm Drug Dispos. 27 (2006) 93–102, https://doi.org/10.1002/bdd.487.

[17] A.A. Sultan, G.A. Saad, G.M. El Maghraby, Permeation enhancers loaded bilosomes for improved intestinal absorption and cytotoxic activity of doxorubicin, Int. J. Pharm. 630 (2023), 122427, https://doi.org/10.1016/j.ijpharm.2022.122427.

[18] A.A. Sultan, N.F. El Nashar, S.M. Ashmawy, G.M. El Maghraby, Cubosomes for enhancing intestinal absorption of fexofenadine hydrochloride: in situ and in vivo investigation, Int. J. Nanomed. 17 (2022) 3543–3560, 10.2147%2FIJN.S370235.

[19] J.N. Pawar, R.T. Shete, A.B. Gangurde, K.K. Moravkar, S.D. Javeer, D.R. Jaiswar, P. D. Amin, Development of amorphous dispersions of artemether with hydrophilic polymers via spray drying: physicochemical and in silico studies, AJPS (Asian J. Plant Sci.) 11 (2016) 385–395, https://doi.org/10.1016/j.ajps.2015.08.012.

[20] S.A. Yehia, M.S. El-Ridi, M.I. Tadros, N.G. El-Sherif, Enhancement of the oral bioavailability of fexofenadine hydrochloride via Cremophor® El-Based liquisolid tablets, Adv. Pharmaceut. Bull. 5 (2015) 569–581, 10.15171%2Fapb.2015.077.

[21] G.M. Maghraby, A.H. Alomrani, Synergistic enhancement of itraconazole dissolution by ternary system formation with pluronic F68 and hydroxypropylmethylcellulose, Sci. Pharm. 77 (2) (2009) 401–418, https://doi.org/10.3797/scipharm.0901-08.

[22] W. Fan, W. Zhu, X. Zhang, L. Di, The preparation of curcumin sustained-release solid dispersion by hot melt Extrusion—I. Optimization of the formulation, J. Pharmaceut. Sci. 109 (2020) 1242–1252, https://doi.org/10.1016/j.xphs.2019.11.019.

[23] J. Szafraniec-Szczęsny, A. Antosik-Rogóż, J. Knapik-Kowalczuk, M. Kurek, E. Szefer, K. Gawlak, K. Chmiel, S. Peralta, K. Niwiński, K. Pielichowski, M. Paluch, R. Jachowicz, Compression-induced phase transitions of bicalutamide, Pharmaceutics 12 (2020) 3390, https://doi.org/10.3390/pharmaceutics12050438.

[24] T.M. Ibrahim, M.H. Abdallah, N.A. El-Megrab, H.M. El-Nahas, Upgrading of dissolution and anti-hypertensive effect of Carvedilol via two combined approaches: self-emulsification and liquisolid techniques, Drug Dev. Ind. Pharm. 44 (2018) 873–885, https://doi.org/10.1080/03639045.2017.1417421.

[25] M.A. Molaei, K. Osouli-Bostanabad, K. Adibkia, J. Shokri, S. Asnaashari, Y. Javadzadeh, Enhancement of ketoconazole dissolution rate by the liquisolid technique, Acta Pharm. 68 (2018) 325–336, https://doi.org/10.2478/acph-2018-0025.

[26] M.M. Ghareeb, A.A. Abdulrasool, A.A. Hussein, M.I. Noordin, Kneading technique for preparation of binary solid dispersion of meloxicam with poloxamer 188, AAPS PharmSciTech 10 (2009) 1206–1215, https://doi.org/10.1208/s12249-009-9316-0.

[27] S.K. Sathigari, V.K. Radhakrishnan, V.A. Davis, D.L. Parsons, R.J. Babu, Amorphous-state characterization of efavirenz—polymer hot-melt extrusion systems for dissolution enhancement, J. Pharmaceut. Sci. 101 (2012) 3456–3464, https://doi.org/10.1002/jps.23125.

[28] A. Chivate, A. Garkal, K. Hariharan, T. Mehta, Exploring novel carrier for improving bioavailability of Itraconazole: solid dispersion through hot-melt extrusion, J. Drug Deliv. Sci. Technol. 63 (2021), 102541, https://doi.org/10.1016/j.jddst.2021.102541.

[29] M.A. Pires, R.A. Souza dos Santos, R.D. Sinisterra, Pharmaceutical composition of hydrochlorothiazide: β-cyclo-dextrin: preparation by three different methods, physico-chemical characterization and in vivo diuretic activity evaluation, Molecules 16 (2011) 4482–4499, https://doi.org/10.3390/molecules16064482.

[30] I. Soppela, S. Airaksinen, M. Murtomaa, M. Tenho, J. Hatara, J. Yliruusi, N. Sandler, Investigation of the powder flow behavior of binary mixtures of microcrystalline celluloses and paracetamol, JEFC 1 (2010) 55–67.

[31] K. Jezsó, P. Peciar, Influence of the selected sieving parameters on the sieving efficiency of material MCC Avicel PH102, J. Mech. Eng. 72 (2022) 77–88, https://doi.org/10.2478/scjme-2022-0008.

[32] R.S. Chaudhary, C. Patel, V. Sevak, M. Chan, Effect of Kollidon VA® 64 particle size and morphology as directly compressible excipient on tablet compression properties, Drug Dev. Ind. Pharm. 44 (2018) 19–29, https://doi.org/10.1080/03639045.2017.1371735.

[33] R.N. Sahoo, A. De, V. Kataria, S. Mallick, Solvent-free hot melt extrusion technique in improving mesalamine release for better management of inflammatory bowel disease, Indian J. Pharm. Educ. Res. 53 (2019) S554–S562, https://doi.org/10.5530/ijper.53.4s.150.

[34] R. Fule, T. Meer, A. Sav, P. Amin, Solubility and dissolution rate enhancement of lumefantrine using hot melt extrusion technology with physicochemical characterisation, J. Pharm. Investig. 43 (2013) 305–321, https://doi.org/10.1007/s40005-013-0078-z.

[35] N. Gao, M. Guo, Q. Fu, Z. He, Application of hot melt extrusion to enhance the dissolution and oral bioavailability of oleanolic acid, Asian J. Pharm. Sci. 12 (2017) 66–72, https://doi.org/10.1016/j.ajps.2016.06.006.

[36] X. Shi, N. Fan, G. Zhang, J. Sun, Z. He, J. Li, Quercetin amorphous solid dispersions prepared by hot melt extrusion with enhanced solubility and intestinal absorption, Pharmaceut. Dev. Technol. 25 (2020) 472–481, https://doi.org/10.1080/10837450.2019.1709502.

[37] S.M. Ashmawy, M.A. Osman, S.A. El-Gizawy, G.M. El Maghraby, D-glucose elicits significant increase in the oral bioavailability of model BCS class III drugs in the rabbit, J. Drug Deliv. Sci. Technol. 49 (2019) 521–526, https://doi.org/10.1016/j.jddst.2018.12.025.

[38] A.A. Sultan, S.A. El-Gizawy, M.A. Osman, G.M. El Maghraby, Self dispersing mixed micelles forming systems for enhanced dissolution and intestinal permeability of hydrochlorothiazide, Colloids Surf. B Biointerfaces 149 (2017) 206–216, https://doi.org/10.1016/j.colsurfb.2016.10.028.

[39] S.M. Ashmawy, S.A. El-Gizawy, G.M. El Maghraby, M.A. Osman, Regional difference in intestinal drug absorption as a measure for the potential effect of P-glycoprotein efflux transporters, J. Pharm. Pharmacol. 71 (2019) 362–370, https://doi.org/10.1111/jphp.13036.

[40] J. Qin, L. Wang, Y. Bai, Y. Li, Y. Jing, L. Han, J. Wang, Enhanced absorption and bioavailability of hydrochlorothiazide by Chinese medicines in the Zhenju antihypertensive compound, J. Pharm. Pharmacol. 66 (2014) 855–864, https://doi.org/10.1111/jphp.12207.

[41] A.A. Sultan, S.A. El-Gizawy, M.A. Osman, G.M. El Maghraby, Colloidal carriers for extended absorption window of furosemide, J. Pharm. Pharmacol. 68 (2016) 324–332, https://doi.org/10.1111/jphp.12516.

[42] A.M. Al-Mohizea, F. Zawaneh, M.A. Alam, F.I. Al-Jenoobi, G.M. El-Maghraby, Effect of pharmaceutical excipients on the permeability of P-glycoprotein substrate, J. Drug Deliv. Sci. Technol. 24 (2014) 491–495, https://doi.org/10.1016/S1773-2247%2814%2950093-7.

[43] J. Huang, L. Si, L. Jiang, Z. Fan, J. Qiu, G. Li, Effect of pluronic F68 block copolymer on P-glycoprotein transport and CYP3A4 metabolism, Int. J. Pharm. 356 (2008) 351–353, https://doi.org/10.1016/j.ijpharm.2007.12.028.

[44] L. Ma, Y. Wei, Y. Zhou, X. Ma, X.A. Wu, Effects of Pluronic F68 and Labrasol on the intestinal absorption and pharmacokinetics of rifampicin in rats, Arch Pharm. Res. (Seoul) 34 (2011) 1939–1943, https://doi.org/10.1007/s12272-011-1114-z.

[45] S.A. Maskarinec, J. Hannig, R.C. Lee, K.Y. Lee, Direct observation of poloxamer 188 insertion into lipid monolayers, Biophys. J. 82 (2022) 1453–1459, 10.1016%2FS0006-3495(02)75499-4.

[46] M.A. Deli, Potential use of tight junction modulators to reversibly open membranous barriers and improve drug delivery, Biochim. Biophys. Acta 1788 (2009) 892–910, https://doi.org/10.1016/j.bbamem.2008.09.016.

[47] H. Yin, H. Shao, J. Liu, Y. Qin, W. Deng, Sex-specific and concentration-dependent influence of Cremophor RH 40 on ampicillin absorption via its effect on intestinal membrane transporters in rats, PLoS One 17 (2022), e0263692, https://doi.org/10.1371/journal.pone.0263692.

[48] Y. Tayrouz, R. Ding, J. Burhenne, K.D. Riedel, J. Weiss, T. Hoppe-Tichy, W. E. Haefeli, G. Mikus, Pharmacokinetic and pharmaceutic interaction between digoxin and Cremophor RH40, Clin. Pharmacol. Ther. 73 (2003) 397–405, https://doi.org/10.1016/s0009-9236(03)00059-6.